View metadata, citation and similar papers at core.ac.uk
brought to you by CORE
provided by Electronic archive of Tomsk Polytechnic University

Structure and thermal behavior of zirconium tungstate under heating

E S Dedova[1,2,3] **E S Shutilova**[1] **R Geber**[4] **L A Gomze**[4] **and S N Kulkov**[1,2,3]
[1]Institute of Strength Physics and Materials Science SB RAS, Tomsk, Russia
[2]National Research Tomsk Polytechnic University, Tomsk, Russia
[3]National Research Tomsk State University, Tomsk, Russia
[4]University of Miskolc, Miskolc, Hungary

E-mail: lsdedova@yandex.ru

Abstract. The morphology and properties of powders $ZrW_2O_7(OH)_2 \cdot 2H_2O$ and ZrW_2O_8, obtained under the conditions of hydrothermal synthesis was studied. Using the high-temperature X-ray analysis, the mechanism of formation of zirconium tungstate was established. The influence of temperature on the structure and properties of materials was studied using shadow-casting method.

1. Introduction

Materials with negative thermal expansion have received attention of researchers in recent decades. Scientific interest determined the establishment of the causes and explanation of the unique thermal behavior of this group of materials. Materials contracting upon heating can solve the technical problem towards the incompatibility of thermal expansion of the constructional design elements. The combination of materials with positive and negative values of thermal expansion in the required ratio allows obtaining materials with low or zero thermal expansion (*so-called invar effect*). The field of application of composite materials is wide and includes such areas as the production of high-precision optical mirrors, thermal protection of descent modules. Additive technology enables the production of ceramic components of complex shape.

Zirconium tungstate is a part of oxide complex system AM_2O_8 (A = Zr, Hf; M = W, Mo). A distinctive characteristic of zirconium tungstate is isotropic compression in a wide temperature range from 0.3 K to 1050 K ($\alpha = -8.6 \cdot 10^{-6}$ K^{-1}) [1]. The thermal behavior of the material is due to the structure. The zirconium tungstate structure is known to consist of ZrO_6 octahedron and WO_4 tetrahedron rigidly connected by a common oxygen atom. With increasing temperature, the oxygen atom in Me - O - Me (Me = Zr, W) bonds starts to oscillate in the transverse direction, which causes the rotation of structural elements, leading to compression of materials [1, 2].

The structure of the zirconium tungstate is strongly affected by the production method as well as by external factors. Promising methods for producing nanosized zirconium tungstate powder are chemical methods, including hydrothermal synthesis. In this case, ZrW_2O_8 powder may be prepared by the controlled decomposition of the $ZrW_2O_7(OH)_2 \cdot 2H_2O$ precursor synthesized at relatively low temperatures. The structure of $ZrW_2O_7(OH)_2 \cdot 2H_2O$ plays an important role in the formation of zirconium tungstate [3, 4] and is very sensitive to preparation conditions. Even minor variation in the production process of the powder has effect on the crystallization process of ZrW_2O_8.

Content from this work may be used under the terms of the Creative Commons Attribution 3.0 licence. Any further distribution of this work must maintain attribution to the author(s) and the title of the work, journal citation and DOI.
Published under licence by IOP Publishing Ltd

Thus, the aims of the work are to study the structure, phase composition and morphology of the precursor and zirconium tungstate powders, to investigate the effect of temperature on the structure and properties of materials, to determine the mechanism of ZrW_2O_8 formation.

2. Experimental procedure

The powder of ZrW_2O_8 was obtained by the thermal decomposition of $ZrW_2O_7(OH)_2 \cdot 2H_2O$ precursor synthesized by the hydrothermal method. The detailed description of the method is given in paper [5].

The specific surface of the powders synthesized was measured by the low-temperature nitrogen adsorption method (BET) [6]. Raw density (ρ_n) was determined by equation: $\rho_n = (m_2-m_1)/V$, where m_1 is the weight of container, m_2 is the weight of container with powder, V is container volume.

The microstructure of ZrW_2O_8 was observed by using Hitachi TM-1000 scanning electron microscope, JEM-2100 transmission electron microscope and MicroVis heating microscope. For this experiment, the powders were compressed into cylindrical samples, which were placed in the installation and heated from room temperature to 1678 K. In microscope, the form of a shadow from samples was fixed, which was used to determine the change of size and shape of simples, wetting angle, the contact angle between the sample and the alumina substrate, on which materials were installed during heating. Scanning was carried out in range of 298–1678 K; the step was 10 K every 10 seconds.

The phase composition and parameters of crystal structure materials was studied using Bruker D8 diffractometer (40 kV, CuKα). Shooting was conducted with the use of standard software and realized in the range of 10 < 2theta < 70 with a step size of 0.02°, acquisition interval 3 c. Temperature ranged from 298 to 1023 K with a step size of 100 K.

3. Results and discussion

Scanning and transmission electron microscopy (SEM and TEM) analysis has shown that $ZrW_2O_7(OH)_2 \cdot 2H_2O$ powder was represented by agglomerates of whisker-like particles and single whisker-like particles (Fig. 1a). The average size in transverse dimension of the particles forming the agglomerates was equal to 50 nm, the average length of single particles was 200 nm. Such shape of the particle was due to the influence of initial components, especially the kind of acid. It is known that the whisker shape of $ZrW_2O_7(OH)_2 \cdot 2H_2O$ particles was determined by the use of hydrochloric acid [3, 7].

The zirconium tungstate powder consisted of whisker-like particles having a block structure. The average block size was up to 50 nm (Fig. 1b). The average transverse size of particles was up to 700 nm; the size in longitudinal direction varied between 500 nm and 5 microns. The particle size distribution was unimodal [8].

Evidently, Figure 1 shows that ZrW_2O_8 crystals inherited the shape and size of $ZrW_2O_7(OH)_2 \cdot 2H_2O$ crystals, except for typical nanosized block structures formed in ZrW_2O_8 particles.

Raw density, characterizing the weight of a unit of freely poured powder, for the two powders was almost similar and was equal to 0.3 g/cm^3. The specific surface area, which characterized the dispersion of powder material, for the two powders was significantly different and was equal to 5.58 m^2/g for ZrW_2O_8 and 19.95 m^2/g for $ZrW_2O_7(OH)_2 \cdot 2H_2O$. Probably, the variation in values of specific surface area was determined by the change in the shape of particles, namely the disappearance of agglomerates in precursor powder and formation of blocks in ZrW_2O_8 particles.

Investigation of the effect of temperature on the structure and properties of powders was carried out using the heating microscope. The obtained images helped to determine contact angle, hot stage of samples and estimate the temperatures of the beginning of sintering, softening, melting and spheroidization processes (Figure 2). The obtained values for $ZrW_2O_7(OH)_2 \cdot 2H_2O$ and ZrW_2O_8 are presented in Table 2.

Samples prepared from precursor powder were sintered at lower temperature (958 K) as compared to ZrW_2O_8 (1240 K). Moreover, this sample sustained higher temperatures and melted at 1431 K in contrast to 1360 K for ZrW_2O_8.

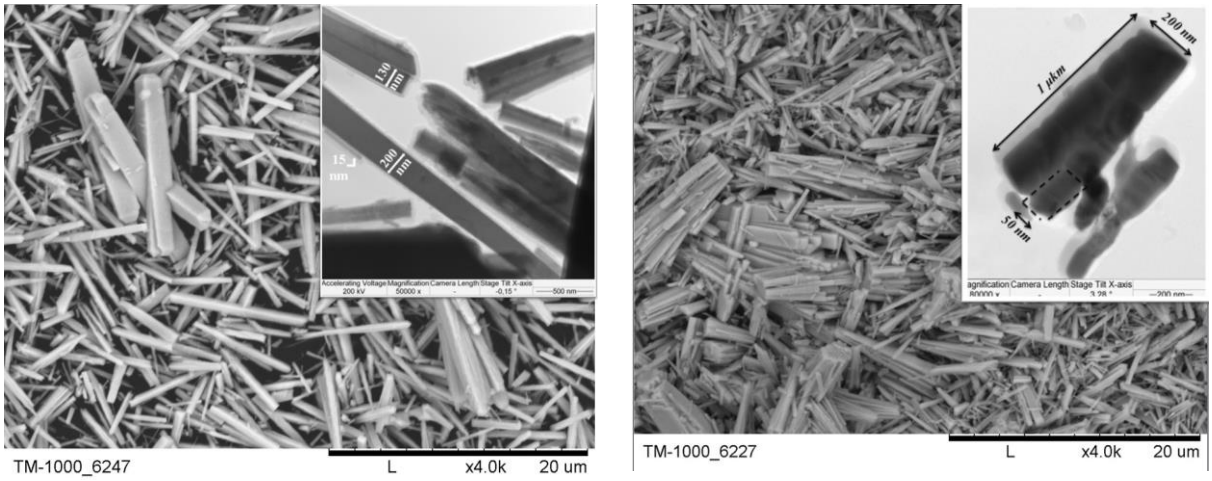

a) b)

Figure 1. The SEM and TEM images of a) $ZrW_2O_7(OH)_2 \cdot 2H_2O$ and b) ZrW_2O_8 powders

Table 1. The characteristics of $ZrW_2O_7(OH)_2 \cdot 2H_2O$ and ZrW_2O_8 powders

Samples	Bulk density, g/cm^3	Specific surface area, m^2/g	Average particle size, μm	
$ZrW_2O_7(OH_1,Cl)_2 \cdot 2H_2O$	0.31	5.58	longitudinal	0.5 - 7
			transverse	0.05 – 0.2
ZrW_2O_8	0.31	19.95	longitudinal	0.5 - 5
			transverse	0.03 – 0.7

While the temperature increased up to 473 K, the monotonic decrease of sample's height $ZrW_2O_7(OH)_2 \cdot 2H_2O$ was noted, which continued up to 1408 K; then, there was a softening of the material. The height of the sample decreased by 37% in relation to its original size. The height of ZrW_2O_8 sample slightly changed with increasing temperature.

The dependence of the change in the wetting angle (θ) of the samples with substrate is shown in Figure 3. According to the plot, the wetting angle was remained almost unchanged up to 900 K. Further increase of the temperature up to 1300 ± 23 K led to the decrease and, subsequently, to the increase of θ values, associated with the deformation of samples upon heating. Obviously, Figure 2 demonstrated the change in the shape of the sample under the influence of temperature; the contact area between the sample and the substrate was decreased, which led to the fluctuation of samples. The subsequent increase of the temperature resulted in a sharp decrease of wetting angles associated with melting of the materials.

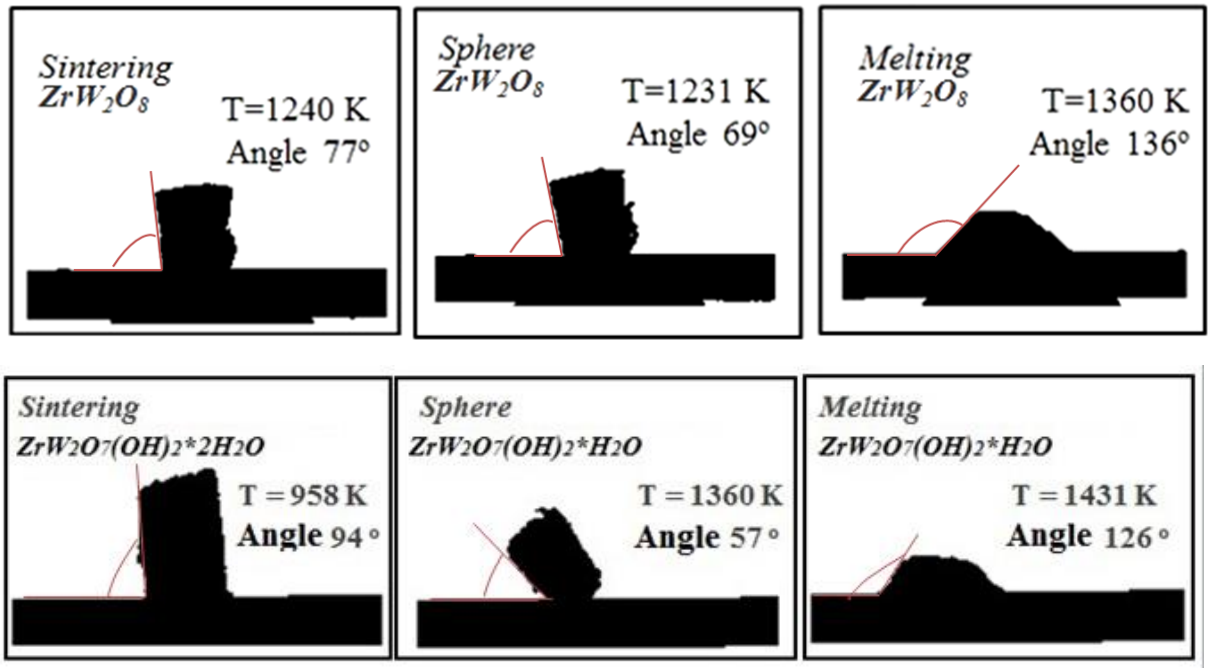

Figure 2. Heating microscopy of the evolution of $ZrW_2O_7(OH)_2 \cdot 2H_2O$ and ZrW_2O_8 samples

Table 2. Temperature data for $ZrW_2O_7(OH)_2 \cdot 2H_2O$ and ZrW_2O_8 samples

Samples	Sintering	Softening	Sphere	½ sphere	Melting
$ZrW_2O_7(OH_1,Cl)_2 \cdot 2H_2O$	958 K	1408 K	1360 K	1405 K	1431 K
ZrW_2O_8	1240 K	1285 K	1231 K	1350 K	1360 K

High-temperature *in situ* X-ray analysis showed that only X-ray peaks of $ZrW_2O_7(OH)_2 \cdot 2H_2O$ were recorded at room temperature [5]. The crystal structure of $ZrW_2O_7(OH)_2 \cdot 2H_2O$ transformed into X-ray amorphous phase above 472 K. The crystal structure corresponding to cubic phase of ZrW_2O_8 was formed up to 873 K. The dependence of the total intensity of all crystalline phases reflexes related to background intensity ($\Sigma I/I_b$) on the temperature in logarithmic coordinates is shown in Figure 4. The resulting dependence was approximated by linear functions; the intersection point of lines corresponding to temperature was equal to 625 K. The comparison of high-temperature X-ray results with thermal analysis carried out earlier [9] has shown that zirconium tungstate was formed by X-Ray amorphous phase at 625 ± 25 K, Fig. 4.

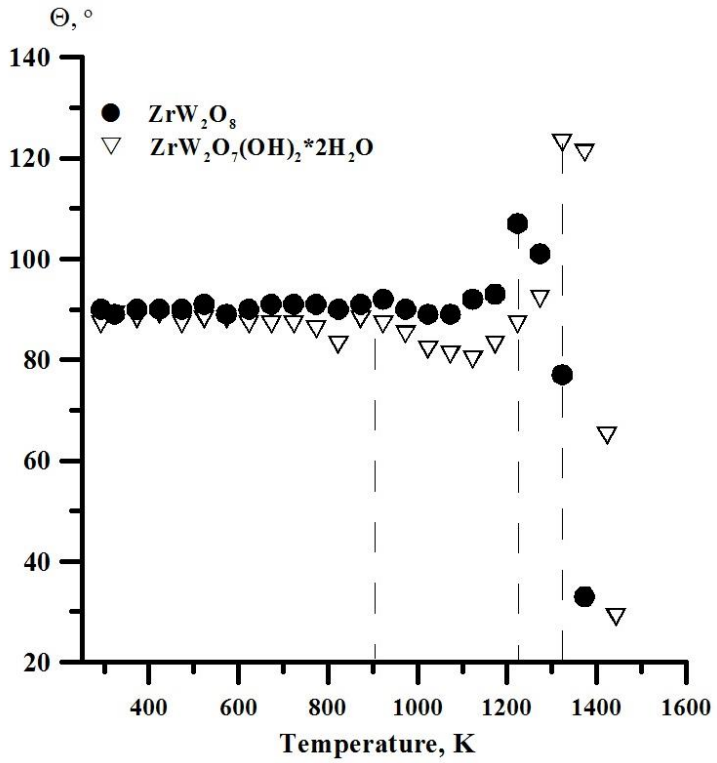

Figure 3. Wetting angle as function of temperature.

Results of high-temperature *in situ* X-ray study of ZrW_2O_8 powder showed solely the peaks of cubic zirconium tungstate in the pattern at room temperature. The heating of the powder above 473 K led to the disappearance of some peaks characteristic to α-ZrW_2O_8. According to [1, 2], the disappearance of some reflexes was due to "order - disorder" phase transformation from low- to high-temperature modifications of zirconium tungstate. Above 823 K, WO_3 and ZrO_2 peaks were recorded in the pattern; their intensity increased with increasing temperature. Reflexes of ZrW_2O_8 were not observed above 1098 K.

The total intensity (ΣI) of ZrW_2O_8 peaks as the function of temperature is shown in Figure 5. As one can see, values ΣI changed with temperature: ΣI decreased from 298 to 473 K, varied within the limits of error from 473 to 823 K and increased above 823 K. The change of total intensity at 473 K corresponded to α → β phase transition, which was accompanied by the disappearance of diffraction maximum. High-temperature cubic phase of zirconium tungsten remained stable up to 823 K. A further increase of temperature led to an increase in the total intensity of X-ray peaks caused by the advent of WO_3 and ZrO_2 peaks. Possibly, at 823 K, ZrW_2O_8 atoms in the lattice started rearranging to form sublattices of ZrO_2 and WO_3, which led to the decomposition of zirconium tungstate to tungsten (VI) oxide and zirconium (IV) oxide above 1098 K.

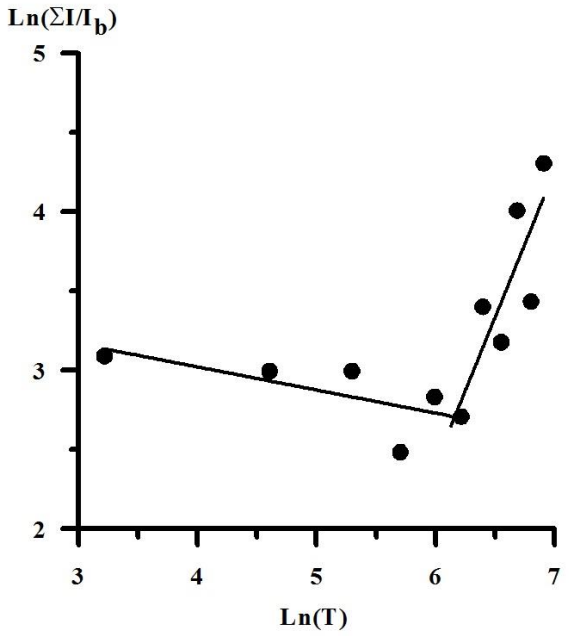

Figure 4. Total intensity of crystal reflections of $ZrW_2O_7(OH)_2 \cdot 2H_2O$ as function of temperature in logarithmic coordinates

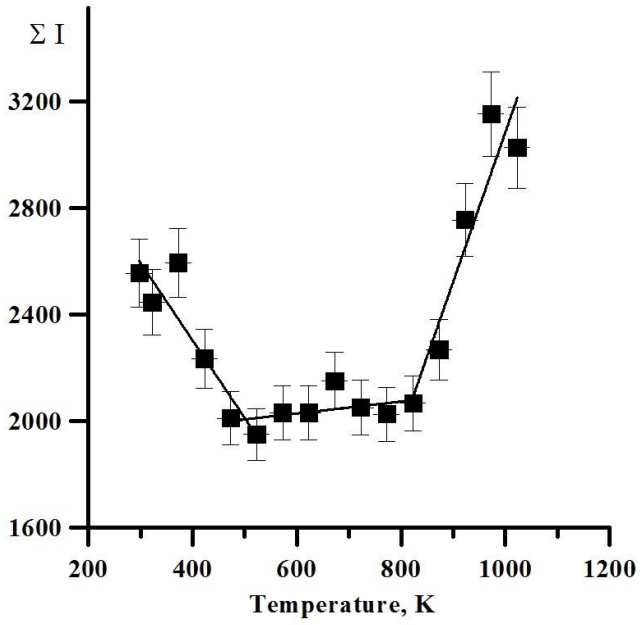

Figure 5. Total intensity of all reflections of ZrW_2O_8 as function of temperature

4. Conclusions

The morphology of $ZrW_2O_7(OH)_2 \cdot 2H_2O$ and ZrW_2O_8 powders was similar and consisted of whisker-like particles, what evidenced the isomorphism of crystals.

The effect of temperature on the structure and properties of powders was investigated. The change of the size and shape of samples, wetting angle, contact angle between the sample and the substrate were determined. It was established that the wetting angle remained almost unchanged up to 900 K. A further increase of the temperature up to 1300 ± 23 K led to the decrease and subsequently the increase of θ values, associated with material spreading on the substrate upon heating.

High-temperature *in situ* X-ray studies have shown that zirconium tungstate was formed through X-Ray amorphous phase at 625 ± 25 K and remained stable from room temperature up to 823 K. Further increase in temperature led to the decomposition of zirconium tungstate caused by the change of the lattice structure by restructuring ZrW_2O_8 atoms to form sublattices of WO_3 and ZrO_2.

Acknowledgements

The research was conducted with partial financial support within the agreement with the Ministry of Education *No. 14.575.21.0040 (RFMEFI57514X0040)*. Transmission electron analysis was obtained using JEM-2100 in the "NANOTECH" Center of ISPMS SB RAS. Study of the morphology (scanning electron microscopy) and thermal behavior (heating microscope) was carried out using analytical equipment of the Miskolc University (Miskolc, Hungary).

References

[1] Mary T A, Evans J S O, Vogt T, Sleight A W 1992 *Science* **272** 90-92
[2] Evans J S O, David W I F, Sleight A W 1999 *Acta Crystallographica* **330** 333–340
[3] Kozy L C, Tahir M N, Lind C, Tremel W 2009 *J Mater Chem* **19** 2760 – 2765
[4] Lind C, Wilkinson A P, Rawb C J, Payzant E A 2001 *J Mater Chem* **11** 3354 - 3359
[5] Gubanov A I, Dedova E S, Plysnin P E and etal 2014 *Thermochimica Acta* **597** 19-26

[6] Greg S and Sing K 1982 *Adsorption Surface Area and Porosity Academic Press*
[7] Badrinarayanan P, Ahmad Md I ,Aknic M, Kessler M R 2011 *Mater Chem. and Phys* **131** 12 – 17
[8] Kulkov S N, Dedova E S, Pedraza F, Erdelyi J 2014 *Epitoanyag - J Sillcate based and Comp Mater* 66(2) 35 - 37
[9] Kulkov S N, Dedova ES, Gubanov A 2013 *I Izv. Vyssh. Ucheb. Zaved. Fizika* **56** 151–156